BIOLOGY OF REPRODUCTION **81,** 33–39 (2009)
Published online before print 18 February 2009.
DOI 10.1095/biolreprod.108.074591

While Dysferlin and Myoferlin Are Coexpressed in the Human Placenta, Only Dysferlin Expression Is Responsive to Trophoblast Fusion in Model Systems[1]

John M. Robinson,[2,3] William E. Ackerman IV,[4] Nicholas J. Behrendt,[4] and Dale D. Vandre[3]

Departments of Physiology and Cell Biology[3] and Obstetrics and Gynecology,[4] The Ohio State University, Columbus, Ohio

ABSTRACT

The syncytiotrophoblast is a specialized epithelium derived from mononuclear cytotrophoblasts that fuse to form this extensive syncytium. Dysferlin is expressed primarily in the apical plasma membrane of the syncytiotrophoblast in the human placenta. Here, we document the presence of another member of the ferlin family, myoferlin, in the placenta and show that it too is expressed primarily in the syncytiotrophoblast. Additionally, we examined the trophoblastic cell lines BeWo, JAR, and JEG-3 for the expression of dysferlin and myoferlin and determined the extent to which their expression was modulated by cell-cell fusion. In trophoblastic cells, there was a positive correlation between cell fusion and increased dysferlin expression but not myoferlin expression. Regarding expression, these trophoblastic cell lines recapitulate the distribution of dysferlin in mononuclear cytotrophoblasts and the syncytiotrophoblast in vivo.

dysferlin, myoferlin, placenta, syncytiotrophoblast, trophoblast

INTRODUCTION

Cell-cell fusion is the cardinal event in the formation of multinucleate syncytia and is part of the normal biology of skeletal muscle, osteoclasts, and the syncytiotrophoblast (STB) layer of the human placenta. Formation of syncytial giant cells also occurs during certain viral infections, such as human immunodeficiency virus. In placenta, the STB is derived from and maintained by mononuclear cytotrophoblasts (CTBs) that fuse with the basal surface of the STB; establishment and maintenance of the STB is crucial for placental function and fetal development [1].

In addition to its formation, other key features of STB biology are its maintenance and turnover during the course of pregnancy. Cytotrophoblasts continue to fuse with the STB throughout pregnancy and replenish its cellular components. It has been estimated that about six times more CTBs fuse with the STB than would be required for its growth [2]. How, then, does the STB accommodate all of the cellular material delivered by the CTBs beyond that required for growth? Nuclei of CTBs gradually become apoptotic after entry into the STB; the time between the incorporation of a CTB nucleus into the STB by fusion and its removal as an apoptotic nucleus is thought to be 3–4 wk [3]. Apoptotic nuclei and cytoplasm in the STB ultimately become clustered into structures called syncytial knots that project from the apical surface of the STB and are subsequently shed from the STB [4, 5]. The number of these shedding events is very large; it has been estimated that a placenta of 12 wk of gestation sheds the equivalent of 1×10^5 CTBs in 4.7×10^4 syncytial knots per day, and the average placenta of 9 mo of gestation sheds 1.8×10^6 CTBs in 8.5×10^5 syncytial knots per day [6]. The underlying cellular and molecular mechanisms controlling syncytial knot formation and shedding, as well as the necessary repair to the plasma membrane of the STB where a syncytial knot breaks away, are not well understood.

Using combined proteomics and cell biological approaches, we found that the protein dysferlin (DYSF) is concentrated in the apical plasma membrane of the STB of term placentas [7]. High expression of DYSF also was found in the STB in first-trimester placentas but was undetectable in the underlying mononuclear CTBs. Moreover, CTBs isolated from term placentas expressed DYSF after spontaneous fusion in culture, whereas nonfused mononuclear cells did not express detectable DYSF [7]. Thus, these in vitro conditions recapitulate the in vivo situation with regard to DYSF expression.

Because we have shown that DYSF is upregulated in a cell fusion-dependent manner in primary trophoblast cultures [7], we hypothesized that DYSF might also be upregulated in a fusion-dependent manner in immortalized trophoblastic cell lines. Based on the identification of myoferlin (MYOF) in our proteomics screen of the STB, we further hypothesized that trophoblast MYOF expression also would be influenced by cell fusion in trophoblasts. In this study, we have extended our examination of DYSF to choriocarcinoma-derived cell lines (BeWo, JAR, and JEG-3 cells) commonly used to model trophoblast cells in vitro. In addition, we have validated the expression of MYOF in term placenta and in trophoblastic cells.

MATERIALS AND METHODS

Reagents

A murine monoclonal antibody to DYSF was purchased from Vector Laboratories (Burlingame, CA). A mouse polyclonal antibody to MYOF was obtained from Novus Biologicals Inc. (Littleton, CO). A rabbit monoclonal antibody to E-cadherin was from Abcam (Cambridge, MA). Horseradish peroxidase-labeled donkey secondary antibodies were obtained from Jackson ImmunoResearch (West Grove, PA). Fluorochrome-labeled goat anti-mouse and anti-rabbit secondary antibodies were from Molecular Probes (Eugene, OR).

Forskolin, dimethyl sulfoxide (DMSO), and a protease inhibitor cocktail (catalog no. P8340) were from Sigma-Aldrich (St. Louis, MO). The cell culture media DMEM/F12 (1:1) containing L-glutamine and 15 mM HEPES, and RPMI medium 1640, medium 199, and DMEM containing L-glutamine were obtained from Gibco-Invitrogen (Grand Island, NY). Fetal bovine serum (FBS), penicillin/streptomycin solution, and trypsin-ethylenediaminetetraacetic acid (trypsin-EDTA) solution were also from Gibco-Invitrogen. The BCA protein determination and SuperSignal chemiluminescent kits were from Pierce

[1]Supported in part by National Institutes of Health grant HD49628.
[2]Correspondence: John M. Robinson, Department of Physiology and Cell Biology, The Ohio State University, 304 Hamilton Hall, 1645 Neil Ave., Columbus, OH 43210. FAX: 614 292 4888;
e-mail: robinson.21@osu.edu

Received: 5 November 2008.
First decision: 20 November 2008.
Accepted: 10 February 2009.
© 2009 by the Society for the Study of Reproduction, Inc.
eISSN: 1259-7268 http://www.biolreprod.org
ISSN: 0006-3363

Downloaded from www.biolreprod.org.

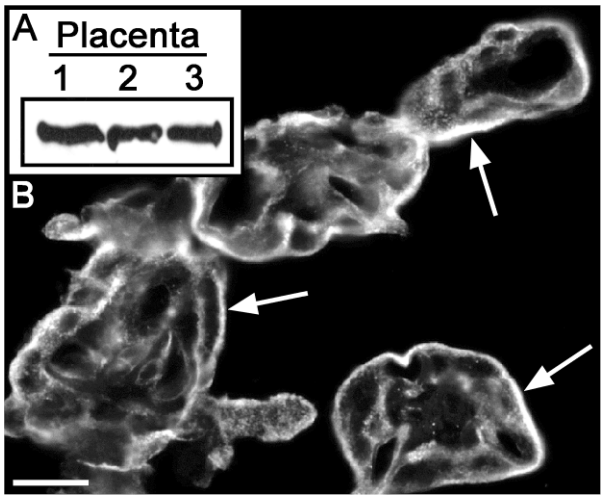

FIG. 1. Expression of myoferlin in the human placenta. **A**) Immunoblot assay for the detection of MYOF. Lysates of three different term placentas were probed, and comparable amounts of MYOF were found in each (equal protein loading in each lane). **B**) Representative IFM localization of MYOF in 5-μm cryostat sections of term placenta. The most intense signal was found in the STB (arrows). Bar = 20 μm.

Biotechnology (Rockford, IL). Scientific imaging film X-OMAT LS was from Eastman Kodak Co. (Rochester, NY). The ProLong antiphotobleaching kit and 4′,6-diamindino-2-phenyindole (DAPI) were obtained from Molecular Probes-Invitrogen (Eugene, OR). TRIzol was from Invitrogen. Tissue-freezing medium for cryosectioning was from Fisher Scientific (Pittsburgh, PA). Other reagents and supplies were as we have described previously [8, 9].

Tissue Collection

Human term placentas were obtained with informed consent according to a protocol approved by the Biomedical Sciences Institutional Review Board of The Ohio State University (Columbus, OH). Tissue samples from uncomplicated cesarean deliveries were used. Tissue was processed as soon as possible after delivery (within 20 min). Placental tissue was either fixed or lysed immediately (see below) or flash frozen in liquid nitrogen and stored at −80°C until it was used. Eight placentas were used in this study.

Cells and Cell Culture

Human-derived BeWo cells, JAR cells, JEG-3 cells, MRC-5 fibroblasts, and HL-60 leukemic cells were obtained from American Type Culture Collection. Primary human umbilical vein endothelial cells (HUVECs) were obtained from Cambrex BioScience (Walkersville, MD). BeWo cells were cultured in DMEM/F12 (1:1) supplemented with 10% FBS, 200 U/ml penicillin, and 200 μg/ml streptomycin. JAR cells were grown in DMEM supplemented with 10% FBS and penicillin/streptomycin. JEG-3 and HL-60 cells were grown in RPMI medium 1640 supplemented with 10% FBS and penicillin/streptomycin. MRC-5 fibroblasts were grown in medium 199 supplemented with 10% FBS and penicillin/streptomycin. Human umbilical vein endothelial cells were grown in a medium optimized for endothelial cells (Cambrex BioScience).

Cells were cultured in tissue culture flasks and maintained at 37°C in a humidified incubator with a 5% CO_2/95% air atmosphere. After reaching ~50% confluence, cells were treated with 20 μM forskolin or the solvent control (0.2% DMSO) for 24, 48, and 72 h. The medium, with forskolin or DMSO, was changed daily over the course of the experiments. HL-60 cells were grown in stationary suspension culture; the medium was changed by centrifuging the cells and resuspending them in fresh control or forskolin-containing media. For microscopy, cells were cultured on 12-mm round coverslips in 24-well culture plates or 22-mm square coverslips in 35-mm Petri dishes. These cells were treated with forskolin or DMSO in the same manner as the cells grown in culture flasks.

Preparation of Tissue and Cell Lysates

Fresh placental tissue or placental tissue frozen previously in liquid nitrogen was cut into small pieces and lysed either 1) by boiling in 1% SDS in 10 mM Tris buffer for 10 min or 2) using octylglucoside lysis buffer (150 mM Na_2PO_4, 60 mM *n*-octyl β-D-glucopyranoside, 10 mM D-gluconic acid lactone, 1 mM EDTA, and 0.02% NaN_3) containing protease inhibitor cocktail. The octylglucoside lysis was carried out on ice for 20 min. Cultured cells were collected by trypsinization for 4 min, and then excess culture medium was added to neutralize the trypsin. The cells were centrifuged, and the pellet was resuspended in and washed with PBS. The cells were pelleted again, and the liquid was aspirated; the cell pellets were flash frozen in liquid nitrogen and stored at −80°C until use. HL-60 cells grew in suspension and did not require trypsination; the washed HL-60 cells were also stored as frozen pellets. The cell pellets were lysed using boiling SDS as described for the tissue samples. The lysates were centrifuged in a microfuge to remove insoluble debris. The protein concentration of placental and cell lysates was determined with the BCA method.

Immunoblot Analysis

Proteins from placental and cell lysates were resolved by SDS-PAGE using 7% acrylamide gels. Proteins separated by gel electrophoresis were transferred electrophoretically to nitrocellulose membranes. The membranes were washed in Tris-buffered saline containing 0.2% Tween 20 (TBST), incubated for 2 h at 22°C with 5% nonfat milk in TBST (TBST/milk) to block nonspecific protein-binding sites, and then incubated overnight at 4°C with primary antibodies in TBST/milk. The antibody dilutions were 1:7500 (anti-DYSF) or 1:1000 (anti-MYOF). After washing in TBST, membranes were incubated with horseradish peroxidase-labeled donkey anti-mouse secondary antibody diluted 1:5000 in TBST/milk for 1 h at 22°C. After washing in TBST, antibody binding was assessed using chemiluminescence and imaging film.

RNA Extraction and RT-PCR

Total RNA was extracted from BeWo cells using TRIzol reagent, according to instructions provided by the manufacturer. RNA was quantified by spectrophotometric absorbance at 260 nm, and 2 μg from each sample was reverse transcribed to cDNA using Superscript III reverse transcriptase and oligo(dT) primers (Invitrogen). Polymerase chain reaction was then performed using Platinum Taq DNA polymerase (Invitrogen) for each set of human-specific primers: DYSF (forward: 5′-ACAGAGGACCAGGGACTCAC; reverse: 5′-CTGCGGTTTGTCTGACAGCA; 177 bp); MYOF (forward: 5′-GACTGTAGCCCTGAAGGAC; reverse: 5′-CCTTATGTTGTTACCACT TAAC; 400 bp); and syncytin-1 (forward: 5′-CCAAGCTCCTTCAGGA GAAC; reverse: 5′-CCATGTGAGGTGGGTTTCC; 405 bp). The amplification conditions for each PCR reaction were as follows: 94°C for 2 min, 28 cycles of denaturation at 94°C (30 sec), annealing at 58°C (30 sec), extension at 72°C (1 min), and final product extension for 5 min at 72°C. Using each primer set, it was confirmed that these reaction conditions were within the linear range of amplification for each product. The identity of all amplification products was verified by sequencing (Plant-Microbe Genomics Facility, The Ohio State University, Columbus, OH). Negative controls were conducted using identical conditions as the test samples, with the exception that reverse transcriptase was omitted; these reactions yielded no amplification products (data not shown). Polymerase chain reaction products were separated by electrophoresis on a 1% agarose gel containing ethidium bromide and visualized using the VersaDoc Imaging System (Bio-Rad).

Immunocytochemistry and Microscopy

Placental tissue and cultured cells were fixed in 4% paraformaldehyde in PBS for 2 h (tissue) or 1 h (cells) at 22°C. The fixed samples were washed extensively with PBS. The washed placental tissue was infiltrated with 20% sucrose in PBS, embedded in tissue-freezing medium, and frozen, and 5-μm cryosections were prepared as we described previously [8]. The sections were incubated with PBS to remove the freezing medium and then incubated with or without 0.5% SDS as we described previously [10]. The SDS treatment is an antigen retrieval procedure important for detecting some antigens in immunocytochemical assays and has been applied to the detection of DYSF [7, 11]. The sections then were washed with four changes of PBS prior to incubation with 5% nonfat milk in PBS for 1 h to block nonspecific protein-binding sites. In immunofluorescence microscopy (IFM) preparations, the sections then were incubated with primary antibodies overnight at 4°C. Anti-DYSF was used at 1:100 or 1:200, whereas anti-MYOF was used at 1:50 or 1:100. The sections were subsequently washed in several changes of PBS over 1 h and then incubated with species-appropriate, fluorochrome-labeled secondary antibody diluted 1:200 for 1 h at 22°C. The cells then were washed several times in PBS, incubated with DAPI for 10 min to label nuclei, washed again, and then mounted in the antiphotobleaching medium. In control

Downloaded from www.biolreprod.org.

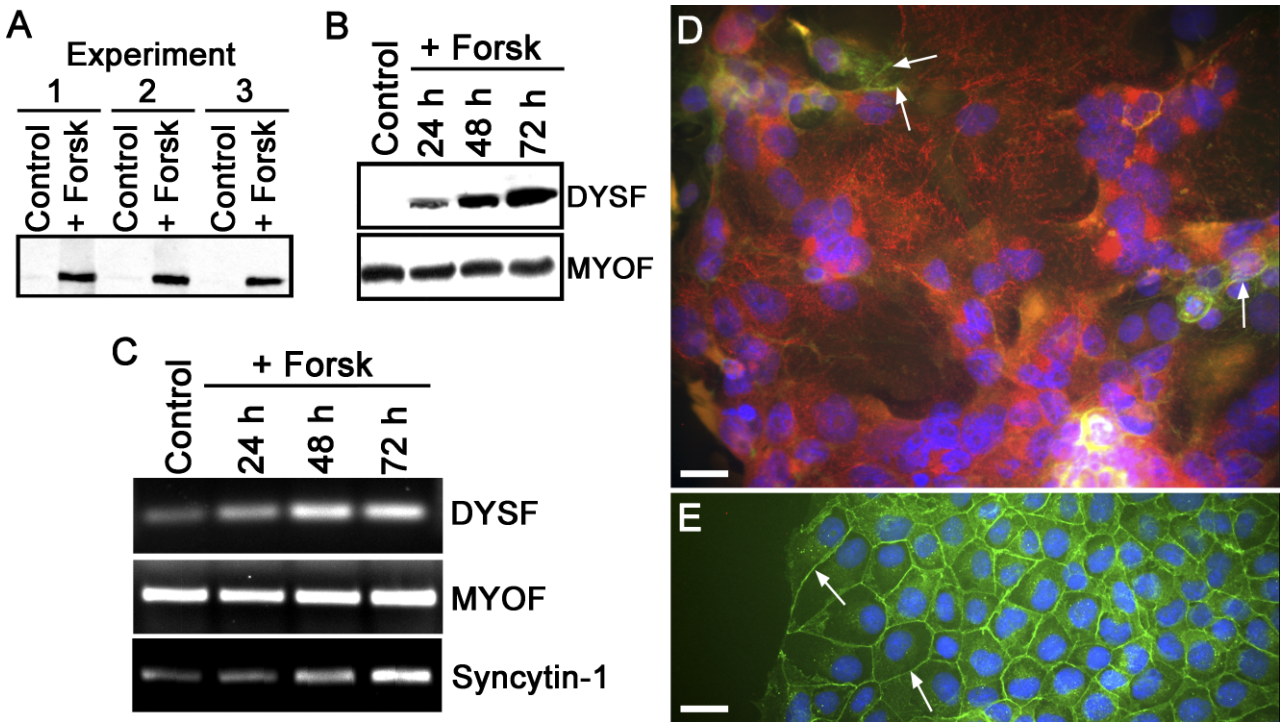

FIG. 2. Dysferlin, but not MYOF, expression is upregulated in fused BeWo cells. **A**) Immunoblot of control and BeWo cells treated with forskolin (Forsk) for three days from three separate experiments. In forskolin-treated BeWo cells, the DYSF signal is dramatically increased in comparison with control samples. Each lane contained 50 μg of protein. **B**) The time course for forskolin-induced upregulation of DYSF was determined. DYSF was detectable by 24 h of forskolin treatment and continued to accumulate at 48 and 72 h. MYOF was not altered by forskolin treatment. Each lane contained 50 μg of protein. These immunoblots are representative of at least three separate experiments. **C**) RT-PCR analysis of DYSF, MYOF, and syncytin-1 mRNA in forskolin-treated BeWo cells. The levels of mRNA for DYSF and syncytin-1 were increased in response to forskolin treatment, whereas the levels for MYOF were unchanged. This gel is representative of three separate experiments. **D**) Detection of DYSF in forskolin-treated (3 days) BeWo cells by IFM. The cells were double labeled for the detection of DYSF (red) and E-cadherin (green). The nuclei were labeled with DAPI (blue). These syncytial structures were demonstrated with certainty because of the absence or incomplete nature of E-cadherin-positive partitions between nuclei in these syncytia and were positively labeled for DYSF. Only small remnants of E-cadherin labeling remain in this syncytium (arrows). **E**) In control cells, E-cadherin labeling was continuous at the periphery of cells (arrows), and they lacked DYSF labeling in interphase mononuclear cells. Bars = 20 μm.

preparations, the primary antibodies were omitted, whereas the secondary antibody incubation was retained. Cells grown on glass coverslips with or without forskolin treatment were incubated in essentially the same manner as the tissue sections. In addition, cells were double labeled with anti-DYSF and anti-E-cadherin (diluted 1:500) to assess syncytia formation [12].

Fluorescence and differential interference contract images were collected with a Nikon Optiphot equipped with a Photometrics Cool Snap *fx* CCD camera (Roper Scientific, Tucson, AZ). Images were captured with the MetaMorph image analysis system (Universal Imaging, Downingtown, PA). All images were collected within the linear response range of the CCD camera.

RESULTS

MYOF Expression in the Placenta

A method for preparing highly enriched preparations of the apical plasma membrane of the STB was developed by Robinson et al. [13]; proteomics analysis revealed that both DYSF and MYOF were present in this placental fraction. Using those findings as a springboard, we validated the expression of MYOF in placentas and determined its localization in that tissue. Immunoblotting was used to validate the proteomics data, which indicated the expression of MYOF in the placenta. Proteins in lysates of three different normal-term placentas were resolved on the same gel, transferred to nitrocellulose, and probed with anti-MYOF. Each of the placentas expressed MYOF, and the level of expression was very similar from one sample to another (Fig. 1A). The predominant site of labeling, as determined by IFM, was the STB, with lesser and more variable labeling of endothelial cells, and as yet unidentified stromal cells (Fig. 1B). These results are similar to those obtained for expression of DYSF in the STB [7] and provide corroborative evidence that DYSF and MYOF are coexpressed in the STB.

DYSF and MYOF Expression in Trophoblastic BeWo Cells: Response to Forskolin-Induced Cell Fusion

We have demonstrated previously that DYSF expression only occurs in primary CTBs isolated from term placentas after syncytia formation [7]. Trophoblastic cell lines were examined for the expression of DYSF to determine whether they behaved similarly to CTBs with regard to DYSF expression. In addition, the expression of MYOF also was monitored during forskolin treatment of BeWo cells. Immunoblot analysis showed that mononuclear BeWo cells expressed little or no DYSF; however, DYSF expression was significantly increased in these cells after forskolin-induced cell-cell fusion (Fig. 2A). Analysis of the time course of DYSF expression after forskolin treatment shows that DYSF was readily detectable after 24 h of forskolin treatment and continued to accumulate at 48 and 72 h of treatment (Fig. 2B). When the gels were overloaded with protein for immunoblot assays, low levels of DYSF expression were detected in the control lanes (data not shown); this is consistent with the observations of others that BeWo fusion occurs spontaneously at low levels [14, 15]. Myoferlin expression, on the other hand, was present in the control BeWo cell population but was not responsive to forskolin

Downloaded from www.biolreprod.org.

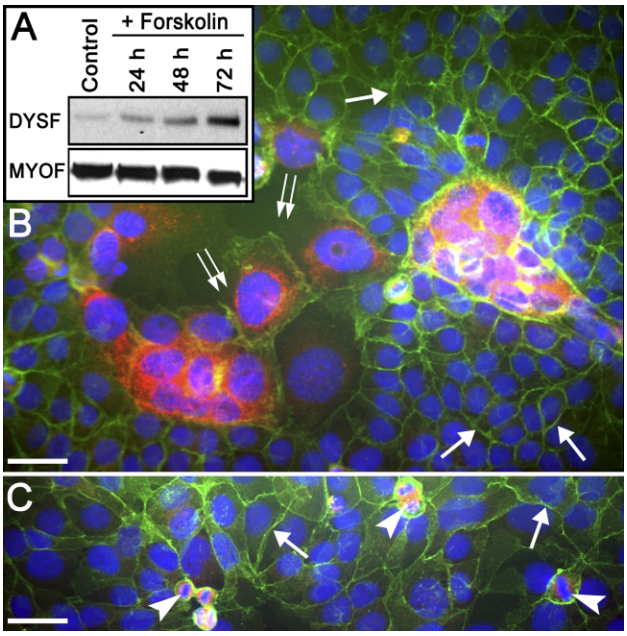

FIG. 3. Dysferlin and MYOF expression in JEG-3 cells. **A**) Immunoblot assay comparing the levels of DYSF and MYOF expression in JEG-3 cells in response to forskolin treatment. Note that there is low but detectable expression of DYSF in the control JEG-3 cells and that this increases with time after forskolin treatment. The levels of MYOF were unchanged by forskolin treatment. These immunoblots are representative of at least three separate experiments. **B**) Detection of DYSF in forskolin-treated (3 days) JEG-3 cells by IFM. The cells were double labeled for the localization of DYSF (red) and E-cadherin (green). Although most cells were not fused, as indicated by the complete band of E-cadherin labeling at the cell periphery (arrows), there were areas where the E-cadherin partitions between nuclei were either missing or incomplete (double arrows), giving rise to multinucleate structures. It was in these multinucleate syncytialike structures that DYSF was detectable. **C**) In control JEG-3 cells, the E-cadherin labeling was intact at the periphery of cells (arrows). Dysferlin was not detectable in these mononuclear interphase cells; however, mitotic cells appeared to be positive (arrowheads), as was the occasional multinucleate structure (not shown). Bars = 20 μm.

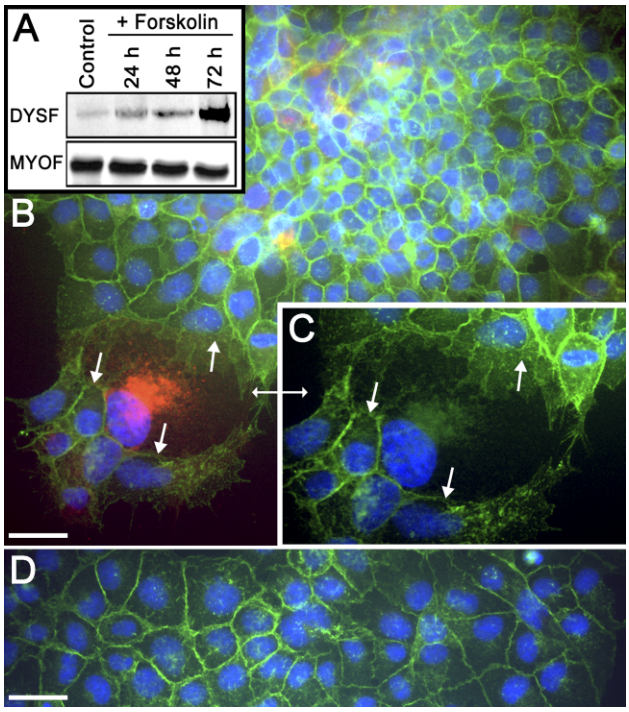

FIG. 4. Dysferlin and MYOF expression in JAR cells. **A**) Immunoblot assay comparing the levels of DYSF expression in JAR cells in response to forskolin treatment. Note that there is low but detectable expression of DYSF in the control JAR cells and that this increases with time after forskolin treatment. The levels of MYOF were unchanged by forskolin treatment. These immunoblots are representative of at least three separate experiments. **B**) Detection of DYSF in forskolin-treated (3 days) JAR cells by IFM. The cells were double labeled for the localization of DYSF (red) and E-cadherin (green). Although most cells were not fused, as indicated by the complete band of E-cadherin labeling at the cell periphery, there were areas where the E-cadherin partitions between nuclei were either missing or incomplete (arrows), giving rise to multinucleate structures. It was in these multinucleate syncytialike structures that DYSF was detectable. **C**) Higher-magnification image of region in **B** denoted by double arrow. Only green and blue fluorescence is shown so that the gaps in E-cadherin labeling are more evident (arrows). Thus, a common cytoplasm is present in this DYSF-positive multinucleate structure. Original magnification ×850. **D**) In control JAR cells, the E-cadherin labeling was intact at the periphery of cells. However, DYSF was not detectable in these interphase mononuclear cells. Bars = 20 μm.

treatment, and MYOF protein levels appeared to remain constant during the course of the experiments (Fig. 2B). Data from RT-PCR experiments demonstrated that DYSF expression was regulated at the mRNA level, as was syncytin-1, another marker of syncytialization that is known to increase in BeWo cells under these conditions (Fig. 2C) [16]. However, MYOF showed no change in mRNA expression in response to forskolin. Cultures of BeWo cells treated with DMSO (controls) or with forskolin also were examined by IFM after double labeling with anti-DYSF and anti-E-cadherin antibodies. Control cells had little, if any, detectable DYSF, whereas BeWo cells in syncytial structures expressed DYSF, even though adjacent nonfused mononuclear cells, whether exposed to forskolin or not, did not express detectable levels of DYSF (Fig. 2, C and D). We also observed that BeWo cells in mitosis appeared to have elevated DYSF compared with adjacent nondividing cells. In the IFM experiments, localization of E-cadherin was used to distinguish between individual cells and syncytia [12]. Syncytial structures could be identified with certainty because unfused cells had a continuous band of E-cadherin labeling at the periphery of cells; E-cadherin labeling was absent or incomplete in the multinucleate fusion products. The present results for DYSF expression in BeWo cells were similar to our previous observations on DYSF expression in the placenta and cultured primary CTBs.

DYSF and MYOF Expression in Trophoblastic JEG-3 and JAR Cells

In contrast to BeWo cells, the trophoblastic cell lines JEG-3 and JAR have not been shown to undergo substantial cell fusion in response to forskolin treatment [17–19]. Therefore, the expression of DYSF in these two cell lines was examined and compared to that found in BeWo cells. Unexpectedly, low but detectable levels of DYSF expression were found in control cultures, and DYSF expression also increased in response to forskolin treatment in a time-dependent manner in both JEG-3 (Fig. 3A) and JAR (Fig. 4A) cells. Similar to the results obtained with BeWo cells, MYOF was expressed in control cells, and MYOF expression in JEG-3 and JAR cells was not responsive to forskolin treatment (Figs. 3A and 4A). Double-labeled IFM of forskolin-treated JEG-3 cells showed the presence of a small number of multinucleate structures compared with control cells. Similar to the results from BeWo cells, these multinucleate structures also labeled positively for DYSF and had reduced E-cadherin labeling. Adjacent nonfused mononuclear cells with continuous E-cadherin labeling

Downloaded from www.biolreprod.org.

did not have detectable DYSF staining, despite being exposed to forskolin (Fig. 3B). Control JEG-3 cultures had continuous E-cadherin labeling at the periphery of cells, with rare multinucleate structures that labeled positively for DYSF (Fig. 3C). Additionally, mitotic cells appeared positive for DYSF expression, whereas interphase mononuclear cells did not have detectable DYSF in our assay. Similarly, DYSF labeling was increased and E-cadherin labeling decreased in occasional multinucleate JAR cells that were present after forskolin treatment, whereas adjacent nonfused mononuclear cells with continuous E-cadherin labeling did not have detectable DYSF (Fig. 4B). Mononuclear control cells had continuous E-cadherin labeling but undetectable DYSF labeling (Fig. 4D). Although neither the JEG-3 nor JAR cells showed extensive cell fusion after forskolin treatment, these results showed that some multinucleate structures were found in response to forskolin treatment. In addition to the low level of expression observed in mitotic cells, increased DYSF expression was restricted to multinucleate and/or fused cells present in all of these trophoblastic cell lines. The IFM signal for DYSF-positive JEG-3 and JAR cells was more intense than in DYSF-positive BeWo cells, suggesting that multinucleate JEG-3 and JAR cells express more DYSF on a per-cell basis than do BeWo cells.

DYSF and MYOF Expression in Nontrophoblastic Cells

A limited number of nontrophoblastic human cells also were tested for the expression of DYSF and MYOF. These were HUVECs, MRC-5 fibroblasts, and HL-60 cells, a leukemic cell line. Cultured HUVECs constitutively expressed DYSF, whereas MRC-5 fibroblasts and HL-60 cells did not have detectable levels of this protein in an immunoblot assay; forskolin treatment did not induce the upregulation of DYSF in either MRC-5 or HL-60 cells (Fig. 5); nor did forskolin treatment induce cell fusion in these cell lines (data not shown). Myoferlin was constitutively expressed in HUVECs and MRC-5 cells but was not detected in HL-60 cells (Fig. 5). It should be noted that two times the protein concentration was used per lane with these cells than with trophoblastic cells (100 μg compared with 50 μg) to optimize for detection of small amounts of DYSF and MYOF.

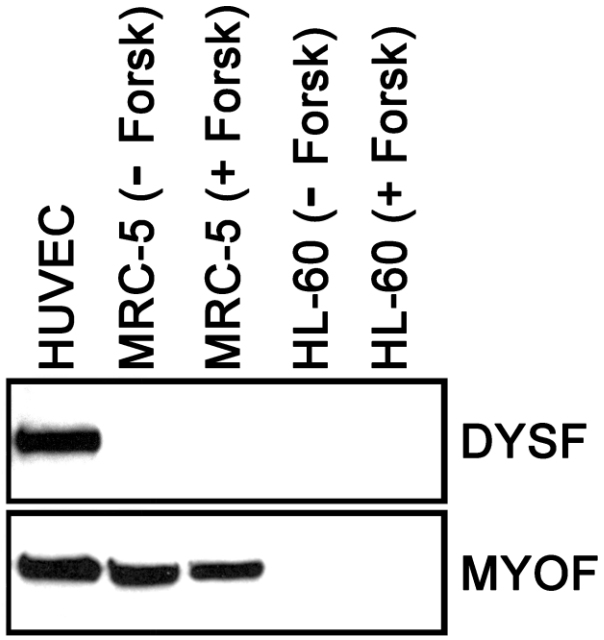

FIG. 5. The expression of DYSF and MYOF was determined in a limited set of nontrophoblastic cells (HUVECs, MRC-5 fibroblasts with or without forskolin [+ Forsk or − Forsk, respectively], and HL-60 cells with or without forskolin) with an immunoblot assay. Human umbilical vein endothelial cells constitutively expressed both DYSF and MYOF, whereas MRC-5 cells did not express DYSF in either control or forskolin-treated cultures but expressed equivalent amounts of MYOF in both conditions. Neither DYSF nor MYOF was detected in control or forskolin-treated HL-60 cells.

DISCUSSION

A proteomics profiling study of a fraction highly enriched in the apical plasma membrane of the STB was noteworthy for the identification of DYSF and MYOF, two plasma membrane proteins previously uncharacterized in the human placenta. In a prior report, we demonstrated that DYSF is expressed in the STB apical plasma membrane of first-trimester and term human placentas but not in CTBs in situ or in primary culture [7]. In the present study, we have extended our consideration of DYSF to other cells, including trophoblastic model systems. Moreover, we have validated the expression of MYOF in the human placenta and have characterized its expression therein and in related cell types. These studies represent the first demonstration of MYOF protein in the human placenta. We have found that the distribution of MYOF in the placenta is similar to that reported previously for DYSF [7], with the STB being the primary site of its localization. In trophoblast-derived cell lines, DYSF expression is only observed after cell-cell fusion, whereas MYOF expression is present in mononuclear cells and remains unchanged after induced (foskolin-treated BeWo cells) syncytialization.

The founding member of the ferlin family of proteins, *fer*-1, was described in the amoeboid sperm of the nematode *Caenorhabditis elegans* within specialized intracellular vesicles important for sperm motility [20]. Based on sequence homology and structural attributes, six mammalian *fer*-1-like proteins have since been identified. Dysferlin (also known as FER1L1) was initially described in skeletal muscle, owing to clinical observations implicating DYSF mutations in limb-girdle muscular dystrophy type 2B and Miyoshi myopathy in humans [21, 22]. Since these initial studies, it also has been demonstrated that DYSF-deficient mice exhibit stress-induced cardiomyopathy [23, 24]. As suggested by our current data, as well as the tissue distribution of DYSF according to the Human Protein Atlas [25], overall expression of DYSF across cell types is limited. Myoferlin, with high sequence homology to DYSF, has been associated with myoblast fusion and myotube formation in skeletal muscle [26, 27]. Compared with wild-type animals, MYOF-deficient mice have an abnormal skeletal muscle phenotype, with small muscle fibers, decreased muscle mass, and impaired regeneration after muscle injury [26]. Outside of skeletal muscle and endothelial cells [28], information regarding the distribution of MYOF in tissues is scanty. We now extend the tissues and cell types known to express MYOF to include human placenta, three trophoblastic cell lines (BeWo, JAR, and JEG-3), and a fibroblast cell line (MRC-5), and confirm its expression in cultured endothelium (HUVECs); however, given that it was not detected in a leukemic cell line (HL-60), our current data suggest that MYOF is not ubiquitously expressed.

The expression patterns for DYSF have been examined in a mouse myoblast cell line (C2C12, with the capacity to differentiate into multinucleate syncytial myotubes in vitro) [29] and in primary human muscle cells [30]. In both of these models, DYSF was poorly expressed prior to the formation of mature myotubes. In the current study, we found that fusion-

Downloaded from www.biolreprod.org.

competent BeWo cells behaved similarly to cultured myoblasts and CTBs with regard to DYSF expression. There was little, if any, DYSF in myoblasts [29, 30], CTBs [7], or mononuclear BeWo cells (present study), whereas upon fusion into syncytial structures, DYSF expression was upregulated in all three systems. It should be noted that low levels of DYSF could be detected in immunoblots of BeWo cells in the absence of forskolin treatment when the gels were overloaded with protein. Low levels of DYSF expression might be anticipated, because it has been reported that BeWo fusion may occur spontaneously in small numbers of the cells depending on culture conditions [13, 14]. We also demonstrated the presence of low levels of spontaneously fused cells in control BeWo cultures. Using double-label IFM, we observed the highest levels of DYSF staining were detected in syncytial structures in BeWo cultures, concomitant with loss of E-cadherin staining. These data on DYSF expression in BeWo cells provide further support for the utility of BeWo cells as a model system to study formation of trophoblastic syncytia. It should be noted that our method of double-label IFM for the simultaneous localization of DYSF and E-cadherin provides a rigorous test for syncytia formation in BeWo cells and can be used to readily distinguish syncytial cells in other trophoblastic cell lines.

In addition to DYSF, the expression of MYOF also has been examined in C2C12 cells. Mononuclear C2C12 myoblasts were found to display high levels of MYOF prior to fusion, whereas protein expression diminished during the process of myotube formation [29]. Contrary to the reciprocal expression of MYOF and DYSF in C2C12 cells, we observed that forskolin-induced syncytial formation did not alter MYOF expression relative to that in prefusion BeWo cells. The significance of the differences in these two cell types with regard to MYOF expression is not known presently. Nevertheless, coexpression of DYSF and MYOF in these fused trophoblastic cells recapitulates the in vivo expression of both proteins in the STB. It has been proposed that formation of skeletal muscle requires at least two distinct steps: myoblast-myoblast fusion and myoblast-myotube fusion, with MYOF being most important for the latter step [27]. Whether the formation of STB, by similarity to the formation of skeletal muscle, requires MYOF awaits further study.

Although BeWo cells are the most proficient at forskolin-induced cell fusion, our results demonstrate that JEG-3 and JAR cells also undergo a modest amount of forskolin-induced multinucleation. Whether this is strictly the result of cell-cell fusion or in part the result of kariokinesis without cytokinesis, as has been observed in JAR cells treated with methotrexate [31], remains to be determined. Most remarkably, in all three trophoblastic cell lines, regardless of their origin, the multinucleate cells contained much higher IFM signals for DYSF than did neighboring mononuclear cells. The signal(s) leading to increased expression of DYSF in fused cells appear to be indirectly related to forskolin because all cells in the cultures were exposed to this compound but mononuclear cells (unfused) did not display elevated levels of DYSF. Rather, it appears that cell fusion itself, or becoming multinucleate, leads to the generation of signals that activate the DYSF gene, which in turn leads to increased expression of the protein DYSF in trophoblastic cells.

In terms of function, both DYSF and MYOF have been implicated in membrane repair. Cell biological studies have shown that DYSF has a role in the rapid repair of damaged plasma membranes in muscle fibers [11, 32] and, more recently, knockdown experiments have further implicated MYOF in the repair of damaged plasma membranes in cultured endothelial cells [28]. Dysferlin-mediated membrane repair is known to require extracellular Ca^{2+} [11, 32], and the structural features and biochemical attributes of DYSF and MYOF indicate that they function as Ca^{2+} sensors. Both DYSF and MYOF contain multiple C2 domains. These regions of about 130 amino acids were initially identified in protein kinase C isoforms. The C2 domains bind anionic phospholipids and proteins in a Ca^{2+}-dependent manner [33, 34]. It is thought that this Ca^{2+}-dependent binding of DYSF to phospholipids and certain proteins is crucial for DYSF to function in membrane repair (reviewed in Glover and Brown [35] and Han and Campbell [36]). Based on these data, both DYSF and MYOF can be considered Ca^{2+}-dependent membrane repair proteins, and we can now speculate that they also function to repair damage to the STB apical plasma membrane as well.

In contrast to observations in skeletal muscle [29, 30], the expression of DYSF and MYOF proteins in the STB is also unique in that both proteins are coincidently expressed at high levels in the same cell. We hypothesize that the apical plasma membrane of the STB is subject to constant damage, both in the form of plasma membrane breaches at sites of syncytial knot shedding and damage secondary to other causes (e.g., traumatic injury). Further, we believe that repair of membrane damage in the STB is likely crucial for placental function, and that both DYSF and MYOF are expressed to ensure prompt membrane repair following injury.

REFERENCES

1. Benirschke K, Kaufmann P. Pathology of the Human Placenta, 4th ed. New York: Springer-Verlag; 2000.
2. Huppertz B, Frank FG, Kingdom JC, Reister F, Kaufmann P. Villous cytotrophoblast regulation of the syncytial apoptotic cascade in the human placenta. Histochem Cell Biol 1998; 110:495–508.
3. Huppertz B, Tews DS, Kaufmann P. Apotosis and syncytial fusion in human placental trophoblast and skeletal muscle. Int Rev Cytol 2001; 205: 215–253.
4. Jones CJ, Fox H. Syncytial knots and intervillous bridges in the human placenta: an ultrastructural study. J Anat 1977; 124:275–286.
5. Martin BJ, Spicer SS. Ultrastructural features of cellular maturation and aging in human trophoblast. J Ultrastruct Res 1973; 43:133–149.
6. Abumaree MH, Stone PR, Chamley LW. An in vitro model of human prophoblast deportation/shedding. Mol Hum Reprod 2006; 12:687–694.
7. Vandré DD, Ackerman WE Jr, Kniss DA, Tewari AK, Mori M, Takizawa T, Robinson JM. Dysferlin is expressed in human placenta but does not associate with caveolin. Biol Reprod 2007; 77:533–542.
8. Lyden TW, Anderson CL, Robinson JM. The endothelium but not the syncytiotrophoblast of human placenta expresses caveolae. Placenta 2002; 23:640–652.
9. Takizawa T, Anderson CL, Robinson JM. A novel Fc gamma R-defined, IgG-containing organelle in placental endothelium. J Immunol 2005; 175: 2331–2339.
10. Robinson JM, Vandré DD. Antigen retrieval in cells and tissues: enhancement with sodium dodecyl sulfate. Histochem Cell Biol 2001; 116:119–130.
11. Bansal D, Miyake K, Vogel SS, Groh S, Chen CC, Williamson R, McNeil PL, Campbell KP. Defective-membrane repair in dysferlin muscular dystrophy. Nature 2003; 423:168–172.
12. Lin L, Xu B, Rote NS. Expression of endogenous retrovirus ERV-3 induces differentiation in BeWo, a choriocarcinoma model of human placental trophoblast. Placenta 1999; 20:109–118.
13. Robinson JM, Ackerman WE, Tewari AK, Kniss DA, Vandre DD. Isolation of highly enriched apical plasma membranes of the placental syncytiotrophoblast. Anal Biochem 2009; 387:87–89.
14. Kudo Y, Boyd CAR, Kimura H, Cook PR, Redman CWG, Sargent IL. Quantifying the syncytialization of human placental trophoblast BeWo cells grown in vitro. Biochim Biophys Acta 2003; 1640:25–31.
15. Rote NS. Intercellular fusion of BeWo. Placenta 2005; 26:686.
16. Kudo Y, Boyd CAR. Changes in expression and function of syncytin and its receptor, amino acid transport system B° (ASCT2), in human placental choriocarcinoma BeWo cells during syncytialization. Placenta 2002; 23: 536–541.
17. Borges M, Bose P, Frank HG, Kaufmann P, Pötgens AJ. A two-color

Downloaded from www.biolreprod.org.

fluorescence assayfor the measurement of syncytial fusion between trophoblast-derived cell lines. Placenta 2003; 24:959–964.
18. Al-Najiry J, Spitz B, Hanssens M, Luyten C, Pijnenborg R. Differential effects of inducers of syncytialization and apotosis on BeWo and JEG-3 choriocarcinoma cells. Hum Reprod 2006; 21:193–201.
19. Vargas A, Morean J, Le Bellego F, Lafond J, Barbean B. Induction of trophoblast cell fusion by a protein tyrosine phosphatase. Placenta 2008; 29:170–174.
20. Achanzar WE, Ward S. A nematode gene required for sperm vesicle fusion. J Cell Sci 1997; 110:1073–1081.
21. Bashir R, Britton S, Strachan T, Keers S, Vafiadaki E, Lako M, Richard I, Marchand S, Bourg N, Argov Z, Sadeh M, Mahjneh I, et al. A gene related to *Caenorhabditis elegans* spermatogenesis factor fer-1 is mutated in limb-girdle muscular dystrophy type 2B. Nat Genet 1998; 20:37–42.
22. Liu J, Aoki M, Illa I, Wu C, Fardeau M, Angelini C, Serrano C, Urtizberea JA, Hentati F, Hamida MB, Bohlega S, Culper EJ, et al. Dysferlin, a novel skeletal muscle gene, is mutated in Miyoshi myopathy and limb girdle muscular dystrophy. Nat Genet 1998; 20:31–36.
23. Han R, Bansal D, Miyake K, Muniz VP, Weiss RM, McNeil PL, Campbell KP. Dysferlin-mediated membrane repair protects the heart from stress-induced left ventricular injury. J Clin Invest 2007; 117:1805–1813.
24. Wenzel K, Geier C, Qadri F, Hubner N, Schulz H, Erdmann B, Gross V, Bauer D, Dechend R, Dietz R, Osterziel KJ, Spuler S, et al. Dysfunction of dysferlin-deficient hearts. J Mol Med 2007; 85:1203–1214.
25. Human Protein Atlas. (URL: http://www.proteinatlas.org/index.php). (November 5, 2008).
26. Davis DB, Delmonte AJ, Ly CT, McNally EM. Myoferlin, a candidate gene and potential modifier of muscular dystrophy. Hum Mol Genet 2002; 9:217–226.
27. Doherty KR, Cave A, Davis DB, Delmonte AJ, Posey A, Earley JU, Hadhazy M, McNally EM. Normal myoblast fusion requires myoferlin. Development 2005; 132:5565–5575.
28. Bernatchez PN, Acevedo L, Fernandez-Hernando C, Murata T, Chalouni C, Kim J, Erdjument-Bromage H, Shah V, Gratton JP, McNally EM, Tempst P, Sessa WC. Myoferlin regulates vascular endothelial growth factor receptor-2 stability and function. J Biol Chem 2007; 282:30745–30753.
29. Davis DB, Doherty KR, Delmonte AJ, McNally EM. Calcium-sensitive phospholipid binding properties of normal and mutant ferlin C2 domains. J Biol Chem 2002; 277:22883–22888.
30. de Luna N, Gallardo E, Soriano M, Dominguez-Perles R, de la Torre C, Rojas-Garcia R, Garcia-Verdugo JM, Illa I. Absence of dysferlin alters myogenin expression and delays human muscle differentiation "in vitro." J Biol Chem 2006; 281:17092–17098.
31. Hochberg A, Rachmilewitz J, Eldar-Geva T, Salant T, Schneider T, de Groot N. Differentiation of choriocarcinoma cell line (JAR). Cancer Res 1992; 52:3713–3717.
32. Lennon NJ, Kho A, Bacskai BJ, Perlmutter SL, Hyman BT, Brown RH Jr. Dysferlin interacts with annexins A1 and A2 and mediates sarcolemmal wound-healing. J Biol Chem 2003; 278:50466–50473.
33. Newton AC. Protein kinase C. Seeing two domains. Curr Biol 1995; 5: 973–976.
34. Nalefeski EA, Falke JJ. The C2 domain calcium-binding motif: structural and functional diversity. Protein Sci 1996; 5:2375–2390.
35. Glover L, Brown RH Jr. Dysferlin in membrane trafficking and patch repair. Traffic 2007; 8:785–794.
36. Han R, Campbell KP. Dysferlin and muscle membrane repair. Curr Opin Cell Biol 2007; 19:409–416.

Downloaded from www.biolreprod.org.